RECONSTRUCTION OF AN 8,000-YEAR RECORD OF TYPHOONS IN THE PEARL RIVER ESTUARY, CHINA

HUANG, G
Department of Environmental Sciences, South China University of Technology, Wushan, Guangzhou 510640, China

YIM, Wyss W-S*
Department of Earth Sciences, The University of Hong Kong, Pokfulam Road, Hong Kong SAR, China

* Presenting author

Summary

An 8,000-year record of typhoons in the Pearl River Estuary is reconstructed through the study of offshore boreholes, beach-dune barriers, historical record and instrumental documentation. In 5 offshore boreholes, a maximum of 17 siliciclastic-dominated storm beds and/or shell-dominated storm beds was identified since about 8,000 calendar years BP. Holocene beach-dune barriers in the vicinity of the estuary were used to study the distribution of landfalling typhoons assisted by radiocarbon and archaeological ages. The pattern found is consistent with multiple typhoons making landfall. Historical record for the period AD 700-1883 has revealed 161 typhoons with reported damage out of which the typhoons of AD 957, 1245, 1862 and 1874 were the most disastrous. During the Little Ice Age, the frequency of typhoons was found to decrease. Only three typhoons in the instrumental documentation period from AD 1884-2000 exceeded the Saffir-Simpson hurricane intensity scale of 3. The frequency of typhoons with paths falling within the South China Sea was found to decrease and increase during El Niño years and La Niña years respectively. Since the mid-1970s, the frequency of typhoons in the South China Sea was found to show a decline probably due to a northerly shift of typhoon paths during El Niño years. However, whether this shift is the result of climate change or natural multidecadal oscillations will require further investigation. Instrumental documentation is concluded to provide the best record of typhoons followed by historical record, beach-dune barriers and offshore boreholes. This is attributed to the inadequate sensitivity of radiocarbon and archaeological ages in distinguishing typhoons and the discontinuous sedimentary record provided by beach-dune barriers and offshore borehole. The degree of damage by typhoons in the historical record is influenced by subjective interpretation.

Keywords
Typhoons, Distribution pattern, Holocene, Pearl River Estuary, Hong Kong, Southern China

1. Introduction

Tropical cyclones are known to kill more people and cause more insured losses than any other natural disaster [MURNANE, 2004]. According to an overview on climate variability and future change by SALINGER [2005], increases in peak wind intensities and the number of tropical cyclones are likely over parts of the world. The vulnerability of coastal regions located along the path of tropical cyclones to damage is therefore likely to be at a maximum where there is rapid population growth and explosive economic development.

Severe tropical cyclones, known as hurricanes in North America and typhoons in eastern Asia, have been the subject of numerous studies on time scales ranging from geological to the present. The study of past tropical cyclones is referred to as paleotempestology [NOTT, 2004; LIU, 2004]. Environments studied have included the mid shelf [e.g. Gagan et al, 1988], the inner shelf [e.g. NELSON, 1982], coastal lakes [LIU and FEARN, 1993] and beach-dune barriers [e.g. HAYNE and CHAPPELL, 2001]. Previous investigations have examined time scales ranging from 5,000 years for radiocarbon dated beach-dune barriers [NOTT and HAYNE, 2001], and by historical documentation in southern China to about 500 years [CHAN and SHI, 2000] and to 1,000 years or more [LIU et al, 2001; LOUIE and LIU, 2003].

In the present study, we attempt to reconstruct the record of typhoons to cover a period of 8,000 years up to AD 2000 using a combination of archives provided by offshore boreholes, beach-dune barriers, historical record and instrumentation documentation. The goal is to compare to different archives and to improve our knowledge on the distribution pattern of typhoons over a longer time scale to assist engineering design and to facilitate disaster planning. We have selected the densely populated and economically important Pearl River Estuary region of southern China for our study. This is followed by an analysis of the typhoon distribution pattern found.

2. Study area

The Pearl River Estuary is located on the northern South China Sea continental shelf just south of the Tropic of Cancer (Fig. 1). Five important advantages of the study area are:
(1) Six either continuously or almost continuously sampled cores with 5 penetrating the Holocene-Pleistocene hiatus [YIM et al, 2004] from a range of water depths down to 26.2 m below Principal Datum (PD - approximately 1.23 m below mean sea level) (Fig. 1) are available for study to identify the number of typhoon-induced storm beds preserved.
(2) Exotic non-estuarine foraminifers introduced into the 'normal' estuarine foraminiferal assemblage during storms [WANG and MURRAY, 1982; HUANG and YIM, 1997] can be used for assisting the recognition of storm mixing together with other sedimentologic properties.
(3) Radiocarbon and archaeological ages of beach-dune barriers in the vicinity of the estuary may provide indication ages of typhoon landfalls in the past [YIM, 1993; YIM and HUANG, 2002].
(4) Typhoon damage for the counties of the Pearl River Delta and vicinity from AD 700-1883 is available from various historical documents kept by the Guangdong Government [HUANG, 2000].
(5) Instrumental documentation of typhoons since 1884 by the Hong Kong Observatory [CHIN, 1972 and other reports] is available. For the present study, we have examined typhoons during the period of documentation from AD 1884-2000.

3. Offshore boreholes

Six boreholes including 3 piston cores (WZ, NL and DEW25) and 3 vibrocores (VB1, PV3 and PV18) (Fig. 1) were used for sedimentological and foraminiferal studies including radiocarbon dating. Magnetic susceptibility measurements were also made on cores VB1, PV3, PV18 and DEW42 to assist the identification of the Holocene-Pleistocene boundary [YIM et al, 2004]. A summary of the radiocarbon ages obtained is shown in Table 1 and the stratigraphy of the cores including seabed depth in metres below PD is shown in Fig. 2. With the exception of core WZ, all cores penetrated the Holocene-Pleistocene boundary and with the exception of core VB1, all cores are continuously sampled. In cores VB1, PV3, PV18 and DEW42, the sharp increases in magnetic susceptibility beneath the Holocene-Pleistocene boundary are accounted for by sub-aerial exposure of the

Pleistocene deposits during the last glacial period [YIM and TOVEY, 1995; TOVEY and YIM, 2002; YIM et al, 2004] (Fig. 2). With the exception of core PV8, the radiocarbon ages from the basal Holocene deposits in all cores except core PV8 are no older than the 8,200 calendar years [YIM, 1999; YIM et al, 2004]. This may be accounted for by the 8,200 calendar year cold event through catastrophic drainage of the Laurentide lakes in north America [Barber et al, 1999; Yim et al, 2006].

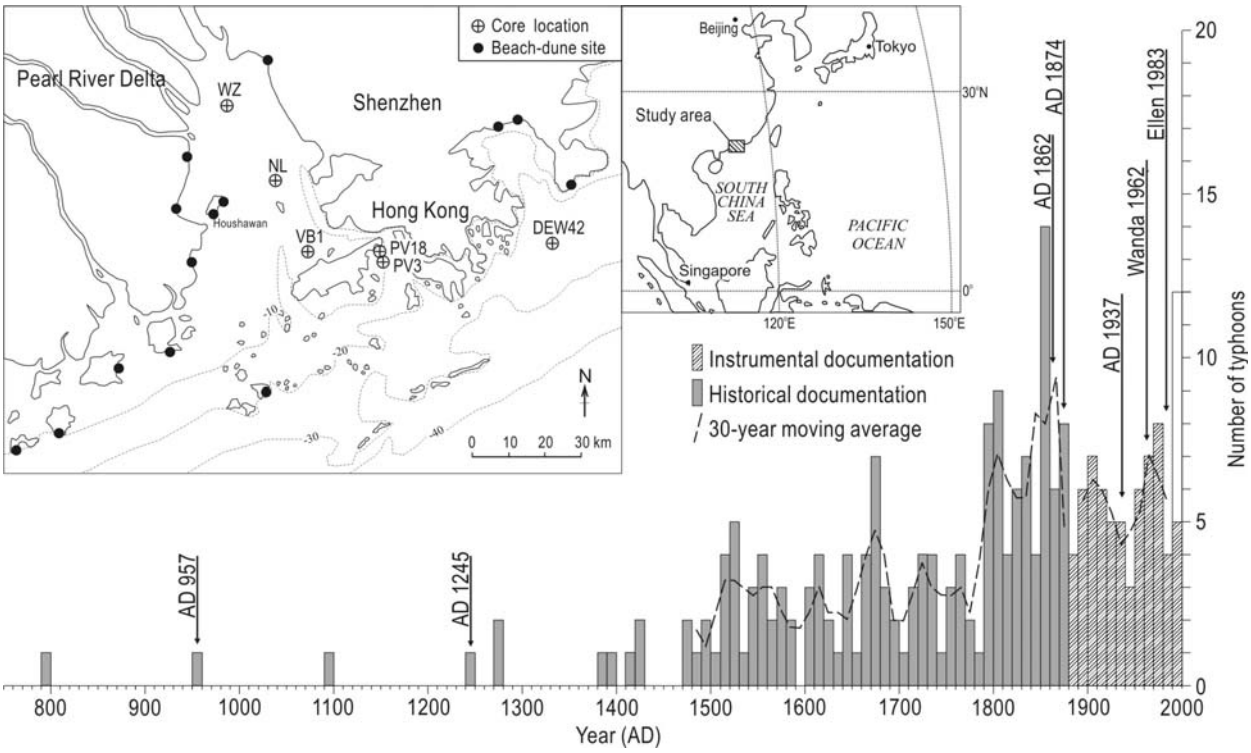

Fig. 1. Location map of the area of study showing the core locations and the beach-dune sites studied, and a plot of the decadal typhoon distribution based on historical documentation before AD1884 and instrumental documentation since AD 1884. The top 7 typhoons during AD957, 1245, 1862, 1874, 1937, 1962 and 1983 are also shown. See text for details.

Five Holocene facies have been identified in the cores including:

(1) Basal transgressive facies of Early-Middle Holocene age

This facies is present in cores NL, VB1 and DEW42. It is a mixture of Holocene and reworked Pleistocene sediments composed of fining upwards clayey siliciclastic sand and shell gravel with plant debris and iron-stained mud pellets representing eroded fragments of the palaeo-desiccated crust formed sub-aerially during the last glacial period [TOVEY and YIM, 2002]. A sharp erosional contact is usually present at the base overlying overconsolidated Pleistocene deposits formed by soil development.

(2) Estuarine facies

This is the most common facies and is found in cores WZ, NL, VB1, PV18 and PV3. It is predominated by clayey silt with shells, shell fragments and plant debris. The molluscs and

foraminifers present are autochthonous in origin and reflected a low energy estuarine environment.

(3) Fluvial-estuarine facies

This facies is present only in the upper 2.5 m of core WZ which is located closest to the river mouths of the Pearl River Delta (Fig. 1). It is a coarsening-upward sequence of clayey silt to clayey siliciclastic-dominated sand indicating the increase in fluvial influence near the river mouths. A radiocarbon age indicates that this facies was formed after 1,613-1,125 calendar years BP.

Core	Water depth (m)	Depth in core (m)	Method[a]	^{14}C age[b]	Calendar age[c]	Sample ID[d]	Material[e]
WZ	6.5	2.7-2.8	C	1 780±110	1 613-1 125	KWG-H9608	mud
		5.3-5.4	C	2 510±130	2 570-1 867	KWG-H9609	mud
NL	6.4	1.1-1.2	C	3 340±110	3 481-2 910	KWG-H9610	mud
		3.3-3.4	C	4 350±120	4 831-4 200	KWG-H9611	mud
		7.5-7.6	C	5 540±120	6 240-5 684	KWG-H9612	mud
		9.9-10	C	6 450±200	7 395-6 517	KWG-H9613	mud
		11.6-11.7	C	20 400±470	-	KWG-H9614	mud
VB1	6.2	0.8-0.9	C	4 480±140	5 047-4 288	ANU-10 154	mud
		6-6.1	C	4 540±190	5 281-4 278	ANU-10 155	mud
		10.2	A	4 740±30	5 187-4 869	KIA-2 287	shell
		11.4-11.5	C	5 440±100	6 058-5 605	ANU-10 156	mud
		12.1-12.2	C	19 430±380	-	ANU-10 157	mud
PV3	7.2	1.5-1.6	C	4 890±200	5 680-4 712	ANU-10 148	mud
		5.5-5.6	C	6 500±110	7 268-6 753	ANU-10 150	mud
		7.5-7.6	C	7 110±120	7 858-7 409	ANU-10 151	mud
		9.5-9.6	C	9 130±240	10 505-9 393	ANU-10 152	mud
		11.8-11.9	C	8 160±180	9 200-8 314	ANU-10 153	mud
PV8	8.3	2..7	A	4 310±40	4 613-4 342	KIA-2288	shell
		10.3	A	7 920±70	8 578-8 267	KIA-2289	shell
DEW42	26	0.5	A	780±30	504-371	KIA-2 290	shell
		1.5	A	1 880±30	1 524-1 364	KIA-2 291	shell
		3.3	A	2 940±30	2 793-2 694	KIA-2 292	shell
		7.25	A	7 490±50	8 096-7 852	KIA-2 293	shell

[a] A – accelerator mass spectrometer; C – conventional.
[b] Results are expressed as radiocarbon conventional ages including δ^{13}C correction.
[c] Calibrated ages obtained using Calib. 4.1 (Stuiver and Reimer, 1993) are given at the 95.4% confidence level (2 sigma) with a reservoir age correction ΔR = -25±20 for the South China Sea in agreement with Southon et al. (2002). The same reservoir age correction were used for shell and organic matter since organic stable carbon isotopic composition indicate that 50-70% of organic carbon originate from marine plankton. Furthermore, terrestrial organic carbon input through rivers is slightly depleted in radiocarbon. The use of this ΔR correction for organic matter is considered to be the most reasonable.
[d] ANU – Australian National University; KIA – Kiel University; GIFA and Gif – CNRS Gif-sur-Yvette.
[e] Sediment organic matter was dated in mud samples.

Table 1 Summary of radiocarbon results obtained from cores WZ, NL, VB1, PV3, PV8 and DEW42.

(4) Open shelf facies

This facies is present only in core DEW42 which is located outside the estuary in the southeastern waters of Hong Kong. It is dominated by homogenous silt with abundant shell remains including foraminifers, echinoids and sponges but is free of terrigenous organic matter.

(5) Storm bed facies

This facies, represented by either siliciclastic-dominated beds or shell-dominated beds, are found interbedded within estuarine mud and fluvial-estuarine sandy mud. They form fining-upwards beds of

up to 40 cm in thickness with a sharp erosional contact at the base. The siliciclastic-dominated storm beds are present only in the inner estuary in the upper part of cores WZ and NL while the shell-dominated storm beds are present in the central and outer parts of the estuary. Both types of storm beds are thought to represent deposits caused by waning currents resulting from passing typhoons. The shell-dominated storm beds contain high concentrations of estuarine molluscs and show bimodal particle-size distribution with a suspension mode and an *in situ* settling mode. During typhoons, the resuspension of mud on the seafloor caused concentration of the siliciclastic-dominated sand and gravel fraction and/or shells and shell fragments. The shell-dominated storm beds are found to show a greater diversity of foraminifers with a wider range of grain size than in the estuarine mud. Open shelf foraminifers present include *Epistominella naraensis* (Kuwano)*, Cibides* spp., *Bulimina marginata* d'Orbigny*, Ammonia compressiuscula* (Brady)*, Schackoinella globosa* (Millet)*, Nonionella* spp., and *Lagena* spp. A settling velocity experiment designed to investigate the mobility of 'smaller' exotic foraminifers and quartz grains has confirmed that the tests were likely to be introduced into the estuary from the open shelf during typhoons [HUANG, 2000].

Storm beds are found only in the cores located within the estuary at a seabed depth of not exceeding 17 m below PD (Fig. 2). This is confirmative of considerable reworking by typhoons in the shallow inner continental shelf. A maximum number of 17 storm beds are found in cores NL and PV18. Based on the two storm beds occurring just below the radiocarbon age of 7,858-7,409 calendar years BP obtained in core PV3, typhoons are likely to have existed since about 8,000 calendar years BP. However, the radiocarbon ages obtained are insufficiently sensitive to identify typhoons at the centennial level of resolution. Furthermore, because of the 'small' number of storm beds preserved in the cores, the storm beds are likely to represent only the younger major typhoons which are preserved. Older major typhoons cannot be preserved because of their destruction by younger major typhoons unless they are sufficiently deeply buried. In core DEW 42, the absence of storm beds may be explained by the 'high' energy open shelf environment of the locality.

In cores VB1, PV3, PV18 and DEW42, an increase in magnetic susceptibility can be seen in the upper part of the core down to a seabed depth of 3 m. This increase in magnetic susceptibility was attributed to shipping contamination over the past 160 years [YIM et al, 2004]. From this, the 10 storm beds identified in the upper 3 m of core PV18 may represents an average of 1 typhoon/16 years. The radiocarbon age of ca. 4,613-4,342 calendar years BP obtained beneath the storm beds is indicative of a hiatus within a few metres of the present seabed with duration of 160-4,600 years. This is attributed to the reworking of seafloor sediments by typhoons during the Late Holocene.

4. Beach-dune barriers

Typhoons landfalling along the coast of the Pearl River Estuary in the past may be indicated by high-level beach rock and beach-dune barriers. The former ranging from 1 m to 20 m above present day sea level occurs on erosional-dominated rocky headlands [Strange, 1986] while the latter occurs in depositional-dominated bays [Yim, 1993]. We have examined 14 beach-dune barrier sites along the coast of the Pearl River Estuary and vicinity (Fig. 1) in order to identify the timing of typhoon landfalls aided by radiocarbon and archaeological ages. This is based on the hypothesis that typhoon landfalls would result in storm surges and the aeolian transportation of supratidal and intertidal beach sediments inland to form dune ridges on the landward side of the beach. The results of the radiocarbon and archaeological ages of the beach-dune barriers are presented elsewhere in Fig. 3 of YIM and HUANG [2002].

Our examination of the 14 beach-dune sites have shown that radiocarbon and archaeological ages

based on Neolithic artifacts obtained may not be consistent with each other either due to differences in sensitivity or to the landfall of multiple typhoons. The oldest radiocarbon age is found to be ca. 8,500 calendar years BP while the oldest archaeological ages are found to be ca. 7,000 calendar years BP. For the time scale, radiocarbon ages are likely to be at the millennial level of sensitivity while archaeological ages may be at the centennial level of sensitivity. The youngest available age of buried artifacts including stone implements, pottery fragments and coinage should therefore provide the age of the typhoon landfall. In any event, the stratigraphy of beach-dune barriers must be studied in detail to rule out a composite origin by multiple typhoon landfalls.

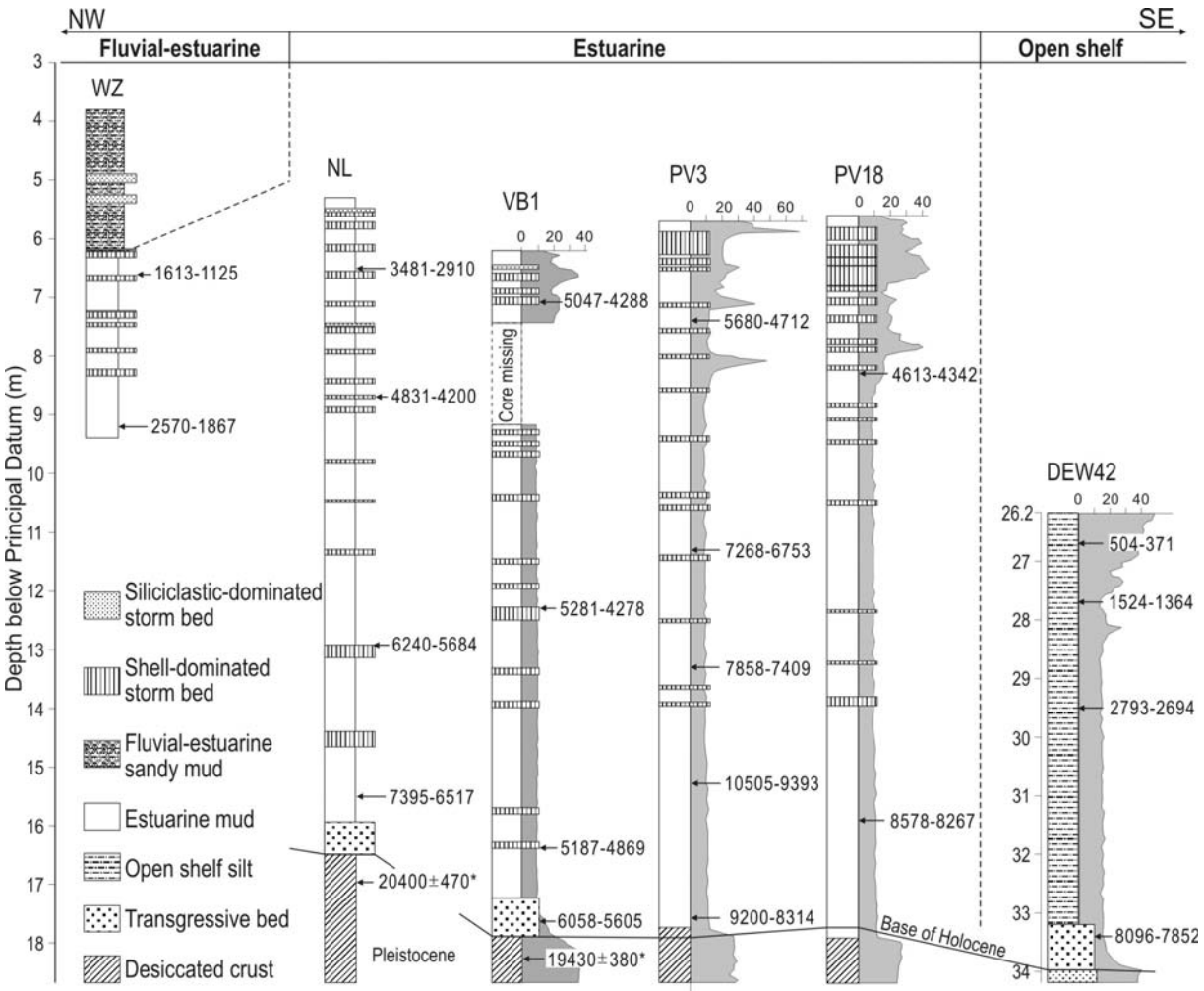

Fig. 2. Stratigraphic section across the Pearl River Estuary showing facies distribution and radiocarbon ages in the 6 cores studied. All radiocarbon ages are calibrated except where marked with an asterisk. Magnetic susceptibility profiles in 10^{-5} SI units are also shown in cores VB1, PV3, PV18 and DEW42.

5. Historical record

The historical documents available for examining typhoons were mainly from government documents

and gazettes of 15 prefectures and counties adjacent to the Pearl River Estuary covering a total area of about 30,000 km^2 [HUANG, 2000]. The AD 700-1883 period examined encompasses the Tang Dynasty (AD 617-907), Song Dynasty (AD 960-1127), Yuan Dynasty (AD 1279-1368), Ming Dynasty (AD 1368-1644) and Qing Dynasty (AD 1644-1911).

Table 2 shows a classification of typhoons in the vicinity of the Pearl River Estuary from AD 700-1883 inferred from reported damage in the historical documents. Based on the number of counties affected and the death toll, the 161 typhoons found may be classified into 3 categories of increasing severity from I to III. Out of these, the 4 most disastrous category III typhoons occurred in AD 957, 1245, 1862 and 1874. The typhoon in AD 957 caused flooding in many settlements including Guangzhou, Panyu, Nanhai, Xinhui and Dongguan. During the AD 1245 typhoon, 9 counties covering about 17,000 km^2 were flooded by seawater and there was a death toll of ca. 10,000. The AD 1862 typhoon brought strong wind lasting about 15 hours, the flooding of 11 counties covering about 25,000 km^2 and a death toll of ca. 80,000. The AD 1874 typhoon caused sea level to rise by ca. 5 m, the flooding of 10 counties covering about 20,000 km^2 and a death toll of ca. 10,000.

Category	No. of counties affected	Damage	No. of typhoons
I	< 4	Moderate to minimal damage to crops and dwellings; death toll < 100	149
II	5-8	Extensive damage to crops and dwellings; death toll 100-5 000	8
III	> 8	Extreme damage to crops and dwellings; death toll > 5 000	4

Table 2 Classification of AD 700-1883 typhoons in the Pearl River Estuary region inferred from historical documentation.

Some doubts exist on the reported damage of typhoons in historical documentation before about AD 1470 because of the lower population density in the Pearl River Estuary region at the time. A lower population density may equate to a lower degree of reported damage for this period. However, this explanation is unlikely for the lower frequency of typhoons found during the 16^{th}-18^{th} century because of the improvement in accuracy of the more recent historical documents.

6. Instrumental documentation

Since 1884, instrumental record of typhoons including barometric pressure, wind velocity and tracks are kept by the Hong Kong Observatory. The record of typhoon tracks before 1960 is nevertheless less accurate because they were determined through mariner's reports. Since 1960, the location of typhoon tracks is improved by the use of radar and satellite imagery.

During AD 1884-2000, only 3 typhoons have been found to exceed the Saffir-Simpson hurricane intensity scale of 3 in terms of the minimum atmospheric pressure (960 mb), maximum sustained wind speed (>50-58 m/sec) and maximum storm surge (>1.7 m). The typhoons were an unnamed typhoon in AD 1937, Typhoon Wanda in AD 1962 and Typhoon Ellen in AD 1982. All 3 typhoons were generated in an area lying east of the Philippines and approached the estuary in a west-north-west direction along

an almost straight path via the Luzon Strait [PETERSEN, 1975; YIM, 1993]. In terms of recurrence interval, Typhoon Ellen is about 1 in 25 years; Typhoon Wanda is about 1 in 50 years, and the unnamed typhoon in 1937 is about 1 in 75 years. The two typhoons with the highest death toll occurred during AD 1906 and AD 1937 with ca. 10,000 (ca. 3 % of the population) and ca. 11,000 (ca. 1 % of the population) respectively.

A total of 132 typhoons were found to pass within a 150-km radius of central Hong Kong with an average frequency of 1.2 times/year. An analysis of the instrumental documentation of typhoons during AD 1946-2000 in the northern South China Sea is presented elsewhere in Fig. 2 of HUANG and YIM [2001]. In this analysis, typhoons in the northwestern Pacific were divided into two groups. One with tracks falling within latitude 10-25^{o}N and longitude 105-120 ^{o}S (the northern South China Sea only) and one with tracks within latitude 0-45^{o}N and longitude 100-160 ^{o}E (the northwestern Pacific including the northern South China Sea). On average about 12 typhoons/year affected the northern South China Sea while about 32 typhoons/year affected the entire northwestern Pacific. By plotting the frequency of typhoons falling within the two areas using 5-year running means, the following conclusions may be drawn:
(a) A decadal oscillation is observed for typhoons in the northern South China Sea.
(b) A 25-year oscillation is observed for typhoons in the northwestern Pacific.
(c) A period of maximum typhoon activity is observed in the northwestern Pacific between 1959 and 1974.
(d) The frequency of typhoons is found to decrease and increase during El Niño years and La Niña years respectively both in the northern South China Sea and the northwestern Pacific.

Based on (d), the decrease in frequency of typhoons shown by the 5-year running mean appears to closely follow El Niño years. The northern South China Sea is found to show a clearer signal than for the northwestern Pacific.

7. Discussion

During the passage of the moderate but fast-moving Typhoon Koryn in 24-28 June, 1993, instrumental documentation of current direction and current velocity by Acoustic Doppler Current Profiler (ADCP) is available from 3 stations located in the outer estuary in the vicinity of core DEW42 (RIDLEY THOMAS 1995, personal communication). Based on the peak wind velocity of greater than 15 m/sec measured, the seawater current velocity exceeded normal conditions by between 3 to 10 times. Consequently, wind-induced currents during typhoons may result in the resuspension of seafloor sediments down to a water depth in excess of 15 m. The increase in exotic foraminifers found in the storm beds within the estuary is therefore likely to be introduced from the open shelf during typhoons.

Figure 1 shows a plot of the decadal typhoon distribution based on historical documentation before AD 1884 and instrumental documentation since AD 1884. For ground-truthing typhoons during the past 8,000 years, instrumental documentation is unquestionably the most reliable because they are based on direct measurements. Historical record is second best because the year of occurrence is accurate. This record is likely to show bias because weaker typhoons during the same year may not have been documented. A problem exists in determining the severity of the typhoon using this record because it is based on the interpretation of the reported damage. Beach-dune barriers are likely to provide a record of typhoon landfalls in low-lying depositional coasts in bay areas where burial ages of artifacts are available. They are absent in highland coasts or where the lowland coasts are protected by man-made dykes. Offshore boreholes located within the estuary are considered to be the least reliable particularly during the Late Holocene because of the discontinuous record caused either by reworking of

subsequent typhoons and/or anthropogenic disturbance of the seabed through shipping and trawling [SELBY and EVANS, 1997]. The inadequate sensitivity of the radiocarbon ages in resolving the age of storm beds and landfall age of typhoons in beach-dune barriers to a decadal or a centennial level is a problem. Nevertheless, beach-dune barriers may possess artifacts such as coinage or burial tombstone to provide a more accurate typhoon landfall age.

Table 3 shows the death toll during major typhoons in the Pearl River Estuary region for the period of historical and instrumental documentation studied. Although the death toll is likely to increase with the severity of the typhoon, this may apply only until the end of the Second World War. Improvements in warning of approaching typhoons through radio and television broadcasts since that time have an important role in the dramatic reduction of the death toll. Furthermore since the 1950s, many of the boat dwellers have abandoned living on boats to settle on land. The estimation of typhoon severity based on the historical documentation of damage is also problematic because unlike instrumental documentation it is not based on maximum wind speed.

Similar to CHAN and SHI [1996], we have found an apparent oscillation in typhoon activity during the period of historical documentation from AD 1470 onwards. The 30-year moving average for decadal typhoons shows an oscillation of the order of 20-30 years (Fig. 1). The period of lower typhoon activity from the mid-14th century to the mid-19th century may be caused by natural variability due to the Little Ice Age [GROVE, 1988].

Year (AD)	Death toll	Year (AD)	Death toll
957	> 10 000	1906	ca. 15 000*
1245	ca. 10 000	1937	ca. 13 000*
1862	ca. 80 000	1962	130*
1874	ca. 10 000	1983	10*

* Death toll in Hong Kong.

Table 3 Death toll during major typhoons in the Pearl River Estuary region for the period of historical and instrumental documentation studied.

A suppressed effect of typhoon activity during El Niño years found in the northwestern Pacific by DONG [1988] is not supported by our findings. The 5-year running mean of typhoon frequency in the northwestern Pacific from 1946-2000 show a very slight decline during El Niño years usually to below 30 times/year [HUANG and YIM, 2001]. This decline in typhoon frequency in the South China Sea during El Niño years is in agreement with the conclusion of ELSNER and LIU [2003] that typhoon tracks shifts northeastwards. From an observational perspective, no significant secular trends have been found for global warming and northwestern Pacific typhoon activity during the decades of reliable records (CHAN and LIU, 2004). In contrast to the increase in tropical cyclone number, duration and intensity found in a warming environment [Webster et al, 2005], no increase in northwestern Pacific category 4-5 typhoon activity was found by Wu et al [2006].

8. Conclusions

Instrumental documentation is found to provide the most accurate and complete record of typhoons followed by historical documentation, beach-dune barriers and offshore boreholes. Nevertheless, it is possible to extend the record of typhoons to 8,000 calendar years BP using a combination of archives. The maximum number of storm beds found to be preserved in 5 boreholes located within the estuary is

17. Radiocarbon carbon dating of core samples and magnetic susceptibility profiling of the cores are indicative of a discontinuous record lasting in duration up to 4,000 calendar years BP within the upper few meters of the seabed. During the period of historical documentation from AD 700-1883, a total of 161 typhoons with reported damage are recorded. Out of these, the 4 most disastrous typhoons occurred in AD 957, 1245, 1862 and 1874. However doubts exist in the record from AD 700-1470 on whether the lower frequency of typhoons documented is real because of the lower population density in the region at the time. Since 1884, 3 typhoons exceeding the Saffir-Simpson hurricane intensity scale of 3 have occurred in 1937, 1962 and 1983.

Radiocarbon ages are found to be insufficiently sensitive in both the offshore boreholes and the beach-dune barriers in distinguishing typhoons at the centennial level of resolution.

For the prediction of future El Niño years, a decrease in the number of typhoons with tracks falling within the South China Sea and an increase in the number of typhoons with tracks outside the South China Sea is found to be useful. In terms of typhoon risk, more typhoons are expected to affect the Pearl River Estuary region during La Niña years. Whether this is a phenomenon of climate change will require further investigation.

Acknowledgements

This work is supported by research grants provided by the National Natural Science Foundation of China and by the Committee on Conference and Research Grants, The University of Hong Kong. The instrumental data on typhoons is provided by the Hong Kong Observatory, Government of the Hong Kong Special Administrative Region. Special thanks are due to Prof. W. N. Ridley Thomas for making available the Acoustic Doppler Current Profiler data for Typhoon Koryn.

References

BARBER, D.C., DYKE, A., HILLAIRE-MARCEL, C., JENNINGS, A.E., ANDREWS, J.T., KERWIN, M.W., BILODEAU, G., MCNEELY, R., SOUTHON, J., MOREHEAD, M.D., GAGNON, J.-M., 1999, Forcing of the cold event of 8200 years ago by catastrophic drainage of Laurentide lakes, *Nature*, v. 400, p344-348.

CHAN, J.C.L., and LIU, S.L., 2004, Global warming and western North Pacific typhoon activity from an observational perspective, *Journal of Climate*, v. 17, p4590-4602.

CHAN, J.C.L., and SHI, J., 1996, Long-term trends and interannual variability in tropical cyclone activity over the western North Pacific, *Geophysical Research Letters*, v. 23, p2765-2768.

CHAN, J.C.L., and SHI, J., 2000, Frequency of typhoon landfall over Guangdong Province of China during the period 1470-1931, *International Journal of Climatology*, v. 20, p183-190.

CHIN, P. C., 1972, Tropical Cyclone Climatology for the China Seas and Western Pacific from 1884 to 1970, v. 1- basic data, *Royal Observatory, Hong Kong Technical Memoirs*, no. 11, 207p.

DONG, K., 1988, El Niño and tropical cyclone frequency in the Australian region and the northwestern Pacific, *Australian Meteorological Magazine*, v. 36/4, p219-255.

ELSNER, J.B., and LIU, K., 2003, Examining the ENSO-typhoon hypothesis, Climate Research, v. 25, p43-54.

GAGAN, M.K., JOHNSON, D.P., and CARTER, R.M., 1988, The cyclone Winifred storm bed, central Great Barrier Reef shelf, Australia, *Journal of Sedimentary Petrology*, v. 58, p845-856.

GROVE, J.M., 1988, *The Little Ice Age*, London, Methuen, 498p.

HAYNE, M., and CHAPPELL, J., 2001, Cyclone frequency during the last 5000 years at Curacoa

Island, north Queensland, Australia, *Palaeogeography Palaeoclimatology Palaeoecology*, v. 168, 207-219.
HUANG, G., 2000, Holocene record of storms in sediments of the Pearl River Estuary and vicinity, *Ph.D. thesis*, Hong Kong, The University of Hong Kong, 353p.
HUANG, G., and YIM, W.W.-S., 1997, Storm sedimentation in the Pearl River Estuary, China, *in* Jablonski, N.G., ed., *The Changing Face of East Asia During the Tertiary and Quaternary*, Hong Kong, Centre of Asian Studies, The University of Hong Kong, p156-177.
HUANG, G., and YIM, W.W.-S., 2001, An 8000-year record of typhoons in the northern South China Sea, *PAGES News*, v. 9/2, p7-8.
LIU, K., 2004, Paleotempestology: principles, methods, and examples from Gulf coast lake sediments, *in* Murnane, R.J., and Liu, K., eds., *Hurricanes and Typhoons*, New York, Columbia University Press, p13-57.
Liu, K., and Fearn, M.L., 1993, Lake-sediment record of late Holocene hurricane activities from coastal Alabama, *Geology*, v. 21, p793-796.
LIU, K., SHEN, C., and LOUIE, K., 2001, A 1,000-year history of typhoon landfalls in Guangdong, southern China, reconstructed from Chinese historical documentary records, *Annals of Association of American Geographers*, v. 91, p453-464.
LOUIE, K., and LIU, K., 2003, Earliest historical records of typhoons in China, *Journal of Historical Geography*, v. 29, p299-316.
MURNANE, R.J., 2004, 1 Introduction, *in* Murnane, R.J., and Liu, K. eds., 2004, *Hurricanes and Typhoons*, New York, Columbia University Press, p1-10.
NELSON, C.H., 1982, Modern shallow-water graded sand layers from storm surges, Bering Shelf, a mimic of Bouma sequences and turbidite systems, *Journal of Sedimentary Petrology*, v. 52, p537-545.
NOTT, J., 2004, Paleotempestology: the study of prehistoric tropical cyclones – a review and implications for hazard assessment, *Environment International*, v. 30, p433-447.
NOTT, J., and HAYNE, M., 2001, High frequency of 'super-cyclones' along the Great Barrier Reef over the past 5,000 years, *Nature*, v. 413, p508-512.
PETERSEN, P., 1975, Storm Surge Statistics, *Tech. Note (Local)*, 20, Royal Observatory, Hong Kong, 20p.
SALINGER, M.J., 2005, Climate variability and change: past, present and future – an overview, *Climate Change*, v. 70, 9-29.
SELBY, I., and EVANS, N.C., 1997, Origins of mud clasts and suspensions on the seabed in Hong Kong, *Continental Shelf Research*, v. 17, p57-78.
SOUTHON, J., KASHGARIAN, M., FONTUGNE, M., METIVIER, B., and YIM, W.W.-S., 2002, Marine reservoir corrections for the Indian Ocean and southeast Asia, *Radiocarbon*, v. 44, p167-180.
STRANGE, P.J., 1986, High level beach rock on Hong Kong Island, *Geological Society of Hong Kong Newsletter*, v. 4/2, p13-16.
STUIVER, M., and REIMER, P.J., 1993, Extended ^{14}C data base and revised calib 3.0 ^{14}C age calibration, *Radiocarbon*, v. 35, p215-230.
TOVEY, N.K., and YIM, W.W.-S., 2002, Desiccation of Late Quaternary inner shelf sediments: microfabric observations, *Quaternary International*, v. 92, p73-87.
WANG, P., and MURRAY, J.W., 1983, The use of foraminifera as indicators of tidal effects in estuarine deposits, *Marine Geology*, v. 51, p239-250.
WEBSTER, P.J., HOLLAND, J.A., CURRY, J.A., and CHANG, H.R., 2005, Changes in tropical cyclones number, duration and intensity in a warming environment, *Science*, v. 309, p1844-1846.
WU, M.-C., YEUNG, K.-H., CHANG, W.-L., 2006, Trends in western north Pacific tropical cyclone intensity, *EOS*, v. 87/48, p537-538.
YIM, W.W.-S., 1993, 22 Future sea level rise in Hong Kong and possible environmental effects, *in* Warrick, R.A., Barrow, E.M., and Wigley, T.M.L. eds., *Climate and Sea level Change: Observations, Projects and Implications*, Cambridge, Cambridge University Press, p349-376.

YIM, W. W.-S., 1999, Radiocarbon dating and the reconstruction of the late Quaternary sea-level changes in Hong Kong, *Quaternary International*, v. 55, p77-91.
YIM, W.W.-S., and HUANG, G., 2002, Middle Holocene higher sea-level indicators from the south China coast, *Marine Geology*, v. 182, p225-230.
YIM, W. W.-S., HUANG, G., and CHAN, L. S., 2004, Magnetic susceptibility study of Late Quaternary inner continental shelf sediments in the Hong Kong SAR, China, *Quaternary International*, v. 117, p41-54.
YIM, W.W.-S., HUANG, G., FONTUGNE, M.R., HALE, R.E., PATERNE, M., PIRAZZOLI, P.A., and RIDLEY THOMAS, W.N., 2006, Postglacial sea-level changes in the northern South China Sea continental shlelf, *Quaternary International*, v. 144, p55-67.
YIM, W.W.-S., and TOVEY, N.K., 1995, Desiccation of inner continental shelf sediments during Quaternary low sea-level stands, *Geoscientist*, v. 5/4, p34-35.